

Acta Crystallographica Section E

Structure Reports

Online

ISSN 1600-5368

Lithium cobalt(II) pyrophosphate, $\text{Li}_{1.86}\text{CoP}_2\text{O}_7$, from synchrotron X-ray powder data

Hui Zhou, Shailesh Upreti, Natasha A. Chernova and
M. Stanley Whittingham*

Chemistry and Materials, SUNY Binghamton, Binghamton, NY, USA

Correspondence e-mail: stanwhit@gmail.com

Received 30 August 2011; accepted 19 September 2011

Key indicators: powder synchrotron study; $T = 297\text{ K}$; mean $\sigma(\text{O}-\text{Li}) = 0.020\text{ \AA}$; disorder in main residue; R factor = 0.057; wR factor = 0.080; data-to-parameter ratio = 91.1.

Structure refinement of high-resolution X-ray powder diffraction data of the title compound gave the composition $\text{Li}_{1.865}\text{CoP}_2\text{O}_7$, which is also verified by the ICP measurement. Two Co sites exist in the structure: one is a CoO_5 square pyramid and the other is a CoO_6 octahedron. They share edges and are further interconnected through P_2O_7 groups, forming a three-dimensional framework, which exhibits different kinds of intersecting tunnels containing Li cations and could be of great interest in Li ion battery chemistry. The structure also exhibits cation disorder with 13.5% Co residing at the lithium (Li1) site. Co seems to have an average oxidation state of 2.135, as obtained from the structural stoichiometry that closely supports the magnetic susceptibility findings.

Related literature

For related structures, see: Adam *et al.* (2008); Nishimura *et al.* (2010); Zhou *et al.* (2011). For related materials with Na^+ and K^+ cations, see: Erragh *et al.* (1991); Sanz *et al.* (1999); Beaury *et al.* (2004); Gopalakrishna *et al.* (2005); Bih *et al.* (2006); Guesmi *et al.* (2007). For related structural frameworks, see: Beaury *et al.* (2004); Fagginani & Calvo (1976); Sandström *et al.* (2003); Etheredge & Hwu (1995); El Maadi *et al.* (1995); Huang & Hwa (1998); Sanz *et al.* (1999); Erragh *et al.* (1998). Pseudovoigt profile coefficients as parameterized in Thompson *et al.* (1987) and Finger *et al.* (1994).

Experimental

Crystal data

$\text{CoLi}_{1.865}\text{O}_7\text{P}_2$
 $M_r = 245.82$
Monoclinic, $P2_1/a$
 $a = 9.76453(4)\text{ \AA}$
 $b = 9.69622(4)\text{ \AA}$

$c = 10.95952(4)\text{ \AA}$
 $\beta = 101.7664(2)^\circ$
 $V = 1015.83(1)\text{ \AA}^3$
 $Z = 8$

Synchrotron radiation,
 $\lambda = 0.413988\text{ \AA}$
 $\mu = 0.89\text{ mm}^{-1}$

$T = 297\text{ K}$
irregular shape, $15 \times 13\text{ mm}$

Data collection

Advanced Photon Source
diffractometer
Specimen mounting: kapton
capillary

Data collection mode: transmission
Scan method: continuous

Refinement

$R_p = 0.057$
 $R_{wp} = 0.080$
 $R_{exp} = 0.049$
 $R(F^2) = 0.04534$

$\chi^2 = 2.624$
24500 data points
269 parameters

Data collection: Advance Photon Source Argonne National Laboratory; cell refinement: *GSAS* (Larson & Von Dreele, 2000); data reduction: *Powder4* (Dragoe, 2001); program(s) used to solve structure: *GSAS*; program(s) used to refine structure: *GSAS*; molecular graphics: *CrystalMaker* (Palmer, 2005); software used to prepare material for publication: *pubCIF* (Westrip, 2010).

Use of the Advanced Photon Source at the Argonne National Laboratory was supported by the US Department of Energy, Office of Science, Office of Basic Energy Sciences, under Contract No. DE-AC02-06CH11357. The research at Binghamton was supported by the Assistant Secretary for Energy Efficiency and Renewable Energy, Office of Vehicle Technologies of the US Department of Energy under Contract No. DE-AC02-05CH11231, under the Batteries for Advanced Transportation Technologies (BATT) Program subcontract # 6807148.

Supplementary data and figures for this paper are available from the IUCr electronic archives (Reference: BR2175).

References

- Adam, L., Guesdon, A. & Raveau, B. (2008). *J. Solid State Chem.* **181**, 3110–3115.
- Beaury, L., Derouet, J., Binet, J., Sanz, F. & Ruiz-Valero, C. (2004). *J. Solid State Chem.* **177**, 1437–1443.
- Bih, H., Saadoun, I. & Mansori, M. (2006). *Moroc. J. Condens. Matter*, **7**, 74–76.
- Dragoe, N. (2001). *J. Appl. Cryst.* **34**, 535.
- El Maadi, A., Boukhari, A. & Holt, E. M. (1995). *J. Chem. Crystallogr.* **25**, 531–536.
- Erragh, F., Boukhari, A., Elouadi, B. & Holt, E. M. (1991). *J. Cryst. Spect. Res.* **21**, 321–326.
- Erragh, F., Boukhari, A., Sadel, A. & Holt, E. M. (1998). *Acta Cryst.* **C54**, 1373–1376.
- Etheredge, K. M. S. & Hwu, S. J. (1995). *Inorg. Chem.* **34**, 1495–1499.
- Fagginani, R. & Calvo, C. (1976). *Can. J. Chem.*, **54**, 3319–3324.
- Finger, L. W., Cox, D. E. & Jephcoat, A. P. (1994). *J. Appl. Cryst.* **27**, 892–900.
- Gopalakrishna, G. S., Mahesh, M. J., Ashamanjari, K. G. & Shashidharaprasad, J. (2005). *J. Cryst. Growth*, **281**, 604–610.
- Guesmi, A., Ouerfelli, N., Mazza, D. & Driss, A. (2007). *Acta Cryst.* **A63**, s277–s278.
- Huang, Q. & Hwu, S. J. (1998). *Inorg. Chem.* **37**, 5869–5874.
- Larson, A. C. & Von Dreele, R. B. (2000). *GSAS*. Report LAUR 86-748. Los Alamos National Laboratory, New Mexico, USA.
- Nishimura, S., Nakamura, M., Natsui, R. & Yamada, A. (2010). *J. Am. Chem. Soc.* **132**, 13596–13597.
- Palmer, D. (2005). *CrystalMaker*. CrystalMaker Software Ltd, Yarnton, England.

Sandström, M., Fischer, A. & Boström, D. (2003). *Acta Cryst.* **E59**, i139–i141.
Sanz, F., Parada, C., Rojo, J. M., Reuiz-Valero, C. & Saez-Puche, R. (1999). *J. Solid State Chem.* **145**, 604–611.

Thompson, P., Cox, D. E. & Hastings, J. B. (1987). *J. Appl. Cryst.* **20**, 79–83.
Westrip, S. P. (2010). *J. Appl. Cryst.* **43**, 920–925.
Zhou, H., Upreti, S., Chernova, N., Hautier, G., Ceder, G. & Whittingham, M. S. (2011). *Chem. Mater.* **23**, 293–300.

supporting information

Acta Cryst. (2011). E67, i58–i59 [https://doi.org/10.1107/S1600536811038451]

Lithium cobalt(II) pyrophosphate, $\text{Li}_{1.86}\text{CoP}_2\text{O}_7$, from synchrotron X-ray powder data

Hui Zhou, Shailesh Upreti, Natasha A. Chernova and M. Stanley Whittingham

S1. Comment

$\text{A}_2\text{MP}_2\text{O}_7$ is a large family, in which various frameworks are encountered consisting of MO_6 octahedra (Fagginani *et al.*, 1976; Sandström *et al.*, 2003) and MO_4 polyhedra (Etheredge *et al.*, 1995; Erragh *et al.*, 1998; Sanz *et al.*, 1999) interconnected through P_2O_7 groups (Fig. 1). Dimeric M_2O_{10} units, built up of two edge-sharing MO_6 octahedra, are only observed for some $\text{A}_2\text{MP}_2\text{O}_7$ pyrophosphates (El Maadi *et al.* 1995; Huang *et al.* 1998) and dimeric M_2O_{11} units (corner-shared MO_6) seem to be much more rare, just observed for $\text{Na}_2\text{CoP}_2\text{O}_7$ (Erragh *et al.* 1991). Two forms of structures were found for $\text{Na}_2\text{CoP}_2\text{O}_7$ by Erragh *et al.* 1991: one is triclinic and another one is orthorhombic. The tetragonal structure of $\text{Na}_2\text{CoP}_2\text{O}_7$ was reported by Sanz *et al.* 1999 and they found that the tetragonal form could be a derivative of the orthorhombic form, with a higher point symmetry for the former. In addition, the tetragonal structured $\text{Na}_2\text{CoP}_2\text{O}_7$ was described by Guesmi *et al.* 2007. To our knowledge, the $\text{A}_2\text{CoP}_2\text{O}_7$ with Li as cation has never been reported.

Here, we report a new Li containing solid with a three-dimensional framework (Fig. 2) crystallizing in the monoclinic space group $P2_1/a$. Its structure is similar to the recently reported $\text{Li}_2\text{MnP}_2\text{O}_7$ (Adam *et al.* 2008), a new member of the $\text{A}_2\text{MP}_2\text{O}_7$ family: original M_2O_6 units, built up of one MO_5 trigonal bipyramid sharing one edge with one MO_6 octahedron, sharing corners with P_2O_7 pyrophosphate groups to form undulating $(\text{M}_4\text{P}_8\text{O}_{32})_\infty$ layers. A 3-D framework results from the interconnection between metal oxide and pyrophosphate groups, and the lithium cations are located in the tunnels thus formed (Fig 2). The structure of the related Fe-compound has been studied by us (Zhou *et al.* 2011) and Nishimura *et al.* (2010), as well as the electrochemical properties, which showed that it is a good candidate for the cathode material of lithium-ion batteries. The title compound also has the potential to work as the cathode material for lithium-ion batteries. We present here its crystal structure, as determined and refined from synchrotron powder X-ray diffraction data (Fig. 3).

S2. Experimental

The powder sample was synthesized through a "wet" method based on mixing stoichiometric aqueous solutions of the precursors followed by thermal treatments. The general procedure involves the mixing of soluble precursors in distilled water followed by a slow evaporation through continuous stirring to dryness before annealing the resultant solids. The precursors for the synthesis were $\text{Li}(\text{CH}_3\text{COO})$, $\text{Co}(\text{CH}_3\text{COO})_2 \cdot 4\text{H}_2\text{O}$, and $\text{NH}_4\text{H}_2\text{PO}_4$, which were dissolved in 100 ml distilled water in a molar ratio of 2:1:2 (1.32 g, 2.49 g and 2.3 g respectively) to give a 0.02 molar lithium solution. The self-adjusted pH of all the solutions were found to be around 4.5. The solution was stirred and evaporated on a hot-plate in the hood followed by vacuum oven drying overnight at 363 K. The resulting solid was preheated in a H_2/He (8.5°/91.5° by volume) atmosphere at 673 K for 4h to decompose the precursors followed by reheating under the same atmosphere up to 873 K for 16h with intermittent grinding to obtain the pink colored powder as final product. The sample was also analyzed with a Perkin-Elmer ICP-OES Optima 7000 DV for the elemental content. The average result of 3

analyses showed that the ratio of Li: Co: P is 1.85: 0.996:2. In addition, the SQUID magnetic study on the sample using a Quantum Design MPMS XL SQUID magnetometer showed that the effective magnetic moment of it is $5.23m_B$ which is typical divalent Co.

S3. Refinement

During structural refinement, occupancy factor for Li1 and Co3 were refined using constrains for atomic coordinate, atomic displacement parameter, and keeping the sum of occupancy factor equals to unity, which later were fixed to their close refined values as 0.73 and 0.27 respectively. Occupancy for Co1 was also observed to be deficient and fixed to it's closely refined value of 0.739 to 0.73, in final refinement cycles.

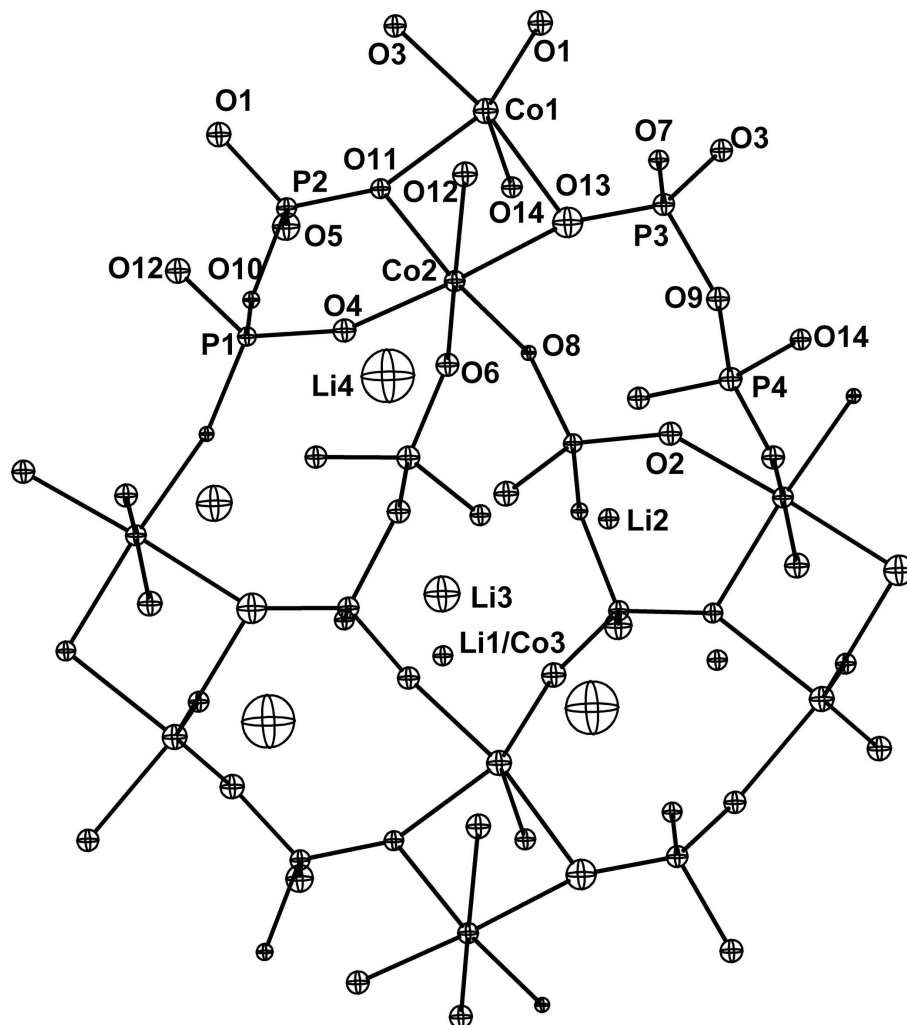


Figure 1

Thermal ellipsoid view of $\text{Li}_{1.86}\text{CoP}_2\text{O}_7$ framework, having edge shared CoO_5 and CoO_6 interconnected through P_2O_7 moieties.

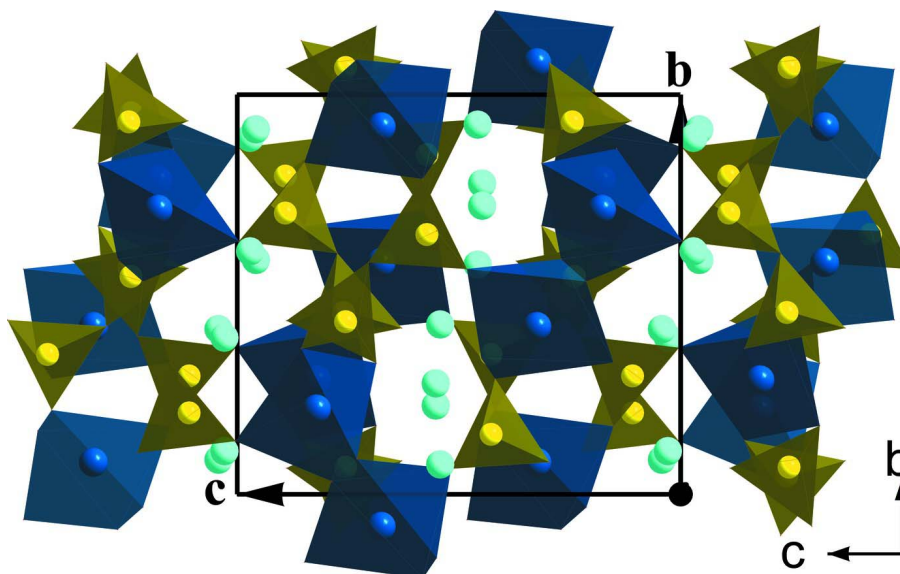


Figure 2

Polyhedral view of unit cell packing showing tunneled structures containing Li ions, viewed along [100].

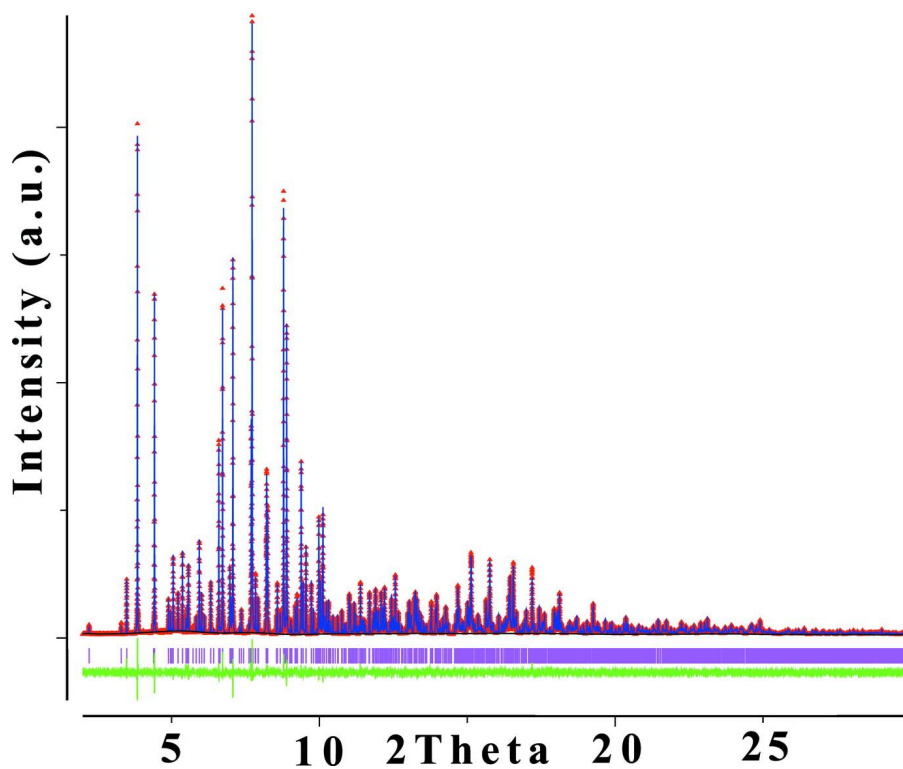


Figure 3

X-ray Rietveld refinement profiles for $\text{Li}_{1.86}\text{CoP}_2\text{O}_7$, data recorded at room temperature. Triangles mark the experimental points (red), solid line is the calculated profile (blue) and bottom trace shows the difference curve (green).

Lithium cobalt(II) pyrophosphate

Crystal data

CoLi_{1.865}O₇P₂ $M_r = 245.82$ Monoclinic, $P2_1/a$

Hall symbol: -P 2yab

 $a = 9.76453 (4) \text{ \AA}$ $b = 9.69622 (4) \text{ \AA}$ $c = 10.95952 (4) \text{ \AA}$ $\beta = 101.7664 (2)^\circ$ $V = 1015.83 (1) \text{ \AA}^3$ $Z = 8$ $F(000) = 948.7$ $D_x = 3.214 \text{ Mg m}^{-3}$

Melting point: 1023 K

Synchrotron radiation, $\lambda = 0.413988 \text{ \AA}$ $\mu = 0.89 \text{ mm}^{-1}$ $T = 297 \text{ K}$

Particle morphology: block

pink

irregular, $15 \times 13 \text{ mm}$ Specimen preparation: Prepared at 873 K and
101.325 kPa

Data collection

Advanced Photon Source
diffractometer

Radiation source: Synchrotron

Si monochromator

Specimen mounting: kapton capillary

Data collection mode: transmission

Scan method: continuous

Refinement

Least-squares matrix: full

 $R_p = 0.057$ $R_{wp} = 0.080$ $R_{exp} = 0.049$ $R(F^2) = 0.04534$

24500 data points

Excluded region(s): Reflections exceeding 2-
theta 30 were omitted for the ease of
refinement.

Profile function: CW Profile function number 3

with 19 terms Pseudovoigt profile coefficients
as parameterized in Thompson *et al.*, (1987) and
Finger *et al.* (1994).#1(GU) = 6.454 #2(GV) = -0.998 #3(GW) =
0.075 #4(GP) = 0.000 #5(LX) = 0.327 #6(LY) =
0.000 #7(S/L) = 0.0011 #8(H/L) = 0.0014
#9(trns) = 0.00 #10(shift) = 0.0000 #11(stec) =
0.00 #12(pte) = 0.00 #13(sfec) = 0.00 #14(L11)
= 0.067 #15(L22) = 0.070 #16(L33) = 0.058
#17(L12) = 0.010 #18(L13) = 0.010 #19(L23) =
-0.004 Peak tails are ignored where the intensity
is below 0.0010 times the peak Aniso.
broadening axis 0.0 0.0 1.0

269 parameters

0 restraints

 $(\Delta/\sigma)_{max} = 0.03$

Background function: GSAS Background

function number 1 with 36 terms. Shifted
Chebyshev function of 1st kind 1: 165.338 2:
-31.4210 3: -8.19118 4: 6.28432 5: -10.8524 6:
14.3842 7: -8.22810 8: -0.949190 9: 13.3092
10: -14.8044 11: 4.75285 12: -1.09442 13:
-0.739293 14: 5.47743 15: -2.87265 16:
1.05489 17: -3.22764 18: 1.21714 19: 0.537209
20: -3.25962 21: 2.18736 22: -1.12437 23:
-2.15219 24: 3.41374 25: -3.88852 26: 1.14500
27: 3.06741 28: -3.05038 29: 0.529274 30:
0.298855 31: -4.06399 32: 1.50867 33: 1.15056
34: -2.20673 35: 0.550944 36: 5.540140E-02

Special details

Experimental. Data was collected with powder sample packed in Kapton capillary

Fractional atomic coordinates and isotropic or equivalent isotropic displacement parameters (\AA^2)

	<i>x</i>	<i>y</i>	<i>z</i>	$U_{\text{iso}}^*/U_{\text{eq}}$	Occ. (<1)
Co1	0.25281 (15)	0.71550 (15)	0.18010 (14)	0.0137 (4)*	0.73
Co2	0.30165 (11)	0.43043 (11)	0.32719 (10)	0.0095 (3)*	
P1	0.3790 (2)	0.6536 (2)	0.5771 (2)	0.0078 (5)*	
P2	0.0613 (2)	0.9265 (2)	0.24116 (18)	0.0089 (5)*	
P3	0.0210 (2)	0.4551 (2)	0.75861 (19)	0.0103 (5)*	
P4	0.6144 (2)	0.7956 (2)	-0.1113 (2)	0.0117 (6)*	
O1	0.1615 (5)	0.8210 (5)	0.3113 (5)	0.0130 (14)*	
O2	0.4709 (5)	0.7806 (5)	-0.0792 (4)	0.0106 (12)*	
O3	0.3911 (5)	0.8599 (4)	0.1472 (5)	0.0107 (13)*	
O4	0.0302 (5)	0.8437 (5)	0.5592 (4)	0.0116 (14)*	
O5	0.4330 (5)	0.4292 (5)	-0.1033 (4)	0.0168 (13)*	
O6	0.1790 (5)	0.8356 (5)	-0.1511 (4)	0.0115 (13)*	
O7	0.0189 (5)	0.4120 (4)	0.6224 (4)	0.0087 (13)*	
O8	0.1866 (5)	0.2976 (4)	0.4146 (4)	0.0047 (12)*	
O9	0.1013 (5)	0.6017 (4)	0.7747 (4)	0.0116 (13)*	
O10	0.3827 (5)	0.5734 (5)	0.7087 (4)	0.0061 (12)*	
O11	0.4152 (5)	0.5900 (4)	0.2661 (4)	0.0085 (13)*	
O12	0.2775 (5)	0.5646 (5)	0.4803 (4)	0.0134 (13)*	
O13	0.3713 (5)	1.0314 (5)	-0.2124 (5)	0.0205 (15)*	
O14	0.2204 (5)	0.6299 (5)	-0.0018 (4)	0.0094 (13)*	
Li1	1.3433 (3)	0.9255 (3)	-0.0397 (3)	0.0087 (7)*	0.73
Li2	0.0807 (17)	0.1083 (15)	0.0261 (15)	0.009 (4)*	
Li3	0.6728 (15)	0.0711 (14)	0.5465 (14)	0.029 (4)*	
Li4	0.400 (2)	0.246 (2)	0.5725 (17)	0.065 (7)*	
Co3	1.3433 (3)	0.9255 (3)	-0.0397 (3)	0.0087 (7)*	0.27

Geometric parameters (\AA , $^\circ$)

Co1—O1	2.105 (5)	P2—O5 ^v	1.524 (4)
Co1—O3	2.028 (4)	P2—O10 ^{iv}	1.584 (5)
Co1—O11	2.067 (4)	P2—O11 ^{vi}	1.516 (5)
Co1—O13 ⁱ	2.226 (5)	P3—O3 ⁱⁱ	1.514 (5)
Co1—O14	2.123 (5)	P3—O7	1.546 (5)
Co2—O4 ⁱⁱ	2.030 (5)	P3—O9	1.616 (4)
Co2—O6 ⁱ	2.180 (5)	P3—O13 ^{vii}	1.563 (5)
Co2—O8	2.068 (4)	P4—O2	1.519 (5)
Co2—O11	2.091 (4)	P4—O6 ⁱⁱⁱ	1.524 (4)
Co2—O12	2.173 (4)	P4—O9 ^{viii}	1.582 (5)
Co2—O13 ⁱ	2.128 (5)	P4—O14 ⁱⁱⁱ	1.589 (5)
P1—O4 ⁱⁱⁱ	1.529 (5)	Co3—O2 ^{ix}	1.983 (5)
P1—O8 ^{iv}	1.547 (4)	Co3—O3 ^{ix}	2.104 (6)
P1—O10	1.633 (5)	Co3—O6 ^{ix}	2.006 (6)

P1—O12	1.556 (4)	Co3—O13 ^{ix}	2.220 (5)
P2—O1	1.512 (5)	Co3—O14 ^x	2.154 (5)
O1—Co1—O3	100.14 (19)	O8—Co2—O11	169.24 (17)
O1—Co1—O11	111.53 (19)	O8—Co2—O13 ⁱ	96.85 (19)
O1—Co1—O14	145.9 (2)	O11—Co2—O13 ⁱ	83.05 (18)
O3—Co1—O11	90.63 (18)	O8 ^{iv} —P1—O10	108.2 (3)
O3—Co1—O14	94.6 (2)	O8 ^{iv} —P1—O12	109.1 (3)
O11—Co1—O14	98.73 (18)	O10—P1—O12	103.6 (3)
O4 ⁱⁱ —Co2—O8	84.60 (18)	O1—P2—O5 ^v	111.4 (3)
O4 ⁱⁱ —Co2—O11	95.03 (18)	O1—P2—O10 ^{iv}	106.9 (3)
O4 ⁱⁱ —Co2—O13 ⁱ	177.0 (2)	O5 ^v —P2—O10 ^{iv}	104.4 (3)

Symmetry codes: (i) $-x+1/2, y-1/2, -z$; (ii) $-x+1/2, y-1/2, -z+1$; (iii) $x+1/2, -y+3/2, z$; (iv) $-x+1/2, y+1/2, -z+1$; (v) $-x+1/2, y+1/2, -z$; (vi) $x-1/2, -y+3/2, z$; (vii) $x-1/2, -y+3/2, z+1$; (viii) $x+1/2, -y+3/2, z-1$; (ix) $x+1, y, z$; (x) $-x+3/2, y+1/2, -z$.